

Laminar Forced Convection Heat Transfer in the Combined Entry Region of Non-Circular Ducts

Y. S. Muzychka

Asst. Prof.

Faculty of Engineering and Applied Science,
Memorial University of Newfoundland,
St. John's, NF, Canada, A1B 3X5

M. M. Yovanovich

Distinguished Professor Emeritus,
Fellow ASME

Department of Mechanical Engineering,
University of Waterloo,
Waterloo, ON, Canada, N2L 3G1

A new model for predicting Nusselt numbers in the combined entrance region of non-circular ducts and channels is developed. This model predicts both local and average Nusselt numbers and is valid for both isothermal and isoflux boundary conditions. The model is developed using the asymptotic results for convection from a flat plate, thermally developing flows in non-circular ducts, and fully developed flow in non-circular ducts. Through the use of a novel characteristic length scale, the square root of cross-sectional area, the effect of duct shape on Nusselt number is minimized. Comparisons are made with several existing models for the circular tube and parallel plate channel and with numerical data for several non-circular ducts. Agreement between the proposed model and numerical data is within ± 15 percent or better for most duct shapes.

[DOI: 10.1115/1.1643752]

Keywords: Forced Convection, Heat Transfer, Heat Exchangers, Internal, Laminar, Modeling

Introduction

Heat transfer in the combined entry region of non-circular ducts is of particular interest in the design of compact heat exchangers. In these applications passages are generally short and usually composed of cross-sections such as triangular or rectangular geometries in addition to the circular tube or parallel plate channel. Also, due to the wide range of applications, fluid Prandtl numbers usually vary between $0.1 < Pr < 1000$, which covers a wide range of fluids encompassing gases and highly viscous liquids such as automotive oils.

A review of the literature reveals that the only models available for predicting heat transfer in the combined entry region are those of Churchill and Ozoe [1,2] for the circular duct and Baehr and Stephan [3] and Stephan [4] for the circular duct and parallel plate channel. Recently, Garimella et al. [5] developed empirical expressions for the rectangular channel, while numerical data for polygonal ducts were obtained by Asako et al. [6]. Additional data for the rectangular, circular, triangular, and parallel plate channel are available in Shah and London [7], Kakac et al. [8], Rohsenow et al. [9], and Kakac and Yener [10]. A complete review of design correlations is presented later. In addition, data are reported for the circular annulus in [7]. The models reported in this paper are applicable to the annulus, but only for the special cases where both surfaces of the annulus are at the same wall temperature or wall flux condition.

The present work will develop a new model using the Churchill and Usagi [11] asymptotic correlation method. In this method, the special asymptotic solutions of the combined entry problem are used to develop a more general model for predicting heat transfer coefficients in non-circular ducts.

Governing Equations

In order to fully appreciate the complexity of the combined entry problem, the governing equations for each of the three fundamental forced convection problems are reviewed. These are as follows: combined entry or simultaneously developing flow, the thermal entrance problem or Graetz flow, and thermally fully developed flow.

Combined Entry, $0 < Pr < \infty$. In cartesian coordinates the governing equations for an incompressible and constant property fluid in the combined thermal entrance region are [7]:

$$\frac{\partial u}{\partial x} + \frac{\partial v}{\partial y} + \frac{\partial w}{\partial z} = 0 \quad (1)$$

$$u \frac{\partial w}{\partial x} + v \frac{\partial w}{\partial y} + w \frac{\partial w}{\partial z} = -\frac{1}{\rho} \frac{dp}{dz} + \nu \left(\frac{\partial^2 w}{\partial x^2} + \frac{\partial^2 w}{\partial y^2} \right) \quad (2)$$

$$u \frac{\partial T}{\partial x} + v \frac{\partial T}{\partial y} + w \frac{\partial T}{\partial z} = \alpha \left(\frac{\partial^2 T}{\partial x^2} + \frac{\partial^2 T}{\partial y^2} \right) \quad (3)$$

The pressure gradient may be written

$$-\frac{1}{\rho} \frac{dp}{dz} = w_c \frac{dw_c}{dz} \quad (4)$$

where $w_c = w_c(z)$ is the velocity of the inviscid core. The above equations are subject to the no slip condition $w_{\text{wall}} = 0$, the boundedness condition $w(x, y, z) \neq \infty$ along the duct axis, and the initial condition $w(x, y, 0) = \bar{w}$. In cartesian coordinates, one additional equation is required to relate the two components of transverse velocity. To date, very few solutions to this set of equations, Eqs. (1–4), have been obtained.

Fully Developed Hydrodynamic Flow, $Pr \rightarrow \infty$. In cartesian coordinates the governing equation for fully developed laminar flow in a constant cross-sectional area duct is

$$\frac{\partial^2 w}{\partial x^2} + \frac{\partial^2 w}{\partial y^2} = \frac{1}{\mu} \frac{dp}{dz} \quad (5)$$

which represents a balance between the pressure and viscous forces.

If the velocity field develops quickly, then the energy equation in cartesian coordinates for thermally developing laminar flow in ducts of constant cross-sectional area is given by

$$\frac{\partial^2 T}{\partial x^2} + \frac{\partial^2 T}{\partial y^2} = \frac{w}{\alpha} \frac{\partial T}{\partial z} \quad (6)$$

where $w = w(x, y)$ is the fully developed velocity profile. This is the classic Graetz problem for a non-circular duct.

Contributed by the Heat Transfer Division for publication in the JOURNAL OF HEAT TRANSFER. Manuscript received by the Heat Transfer Division March 14, 2003; revision received October 2, 2003. Associate Editor: N. K. Anand.

When the flow becomes thermally fully developed the energy equation may be written in terms of the mixing cup temperature $T_m(z)$, Kays and Crawford [12]

$$\frac{\partial^2 T}{\partial x^2} + \frac{\partial^2 T}{\partial y^2} = \frac{w}{\alpha} \frac{dT_m}{dz} \quad (7)$$

for the uniform wall flux (UWF) condition, and

$$\frac{\partial^2 T}{\partial x^2} + \frac{\partial^2 T}{\partial y^2} = \frac{w}{\alpha} \left(\frac{T_w - T}{T_w - T_m} \right) \frac{dT_m}{dz} \quad (8)$$

for the uniform wall temperature (UWT) condition, where

$$T_m(z) = \frac{1}{\bar{w}A} \int \int_A wT dA \quad (9)$$

Later, a model is developed which utilizes a number of limiting approximate solutions to these equations. These are as follows: fully developed flow, thermally developing flow, and laminar boundary layer flow.

A dimensionless heat transfer coefficient or Nusselt number may be defined as

$$Nu_{\mathcal{L}} = \frac{\bar{q}_w(z) \mathcal{L}}{k(\bar{T}_w(z) - T_m(z))} = \frac{h\mathcal{L}}{k} \quad (10)$$

where $T_m(z)$ is the bulk fluid temperature, $\bar{T}_w(z)$ is the average wall temperature, and $\bar{q}_w(z)$ is the average wall heat flux at any point along the duct. For UWT, $T_w = \text{Constant}$ and for UWF, $q_w = \text{Constant}$.

In terms of the solutions to Eqs. (1–4), the Nusselt number, $Nu_{\mathcal{L}}$, may be defined as follows:

$$Nu_{\mathcal{L}} = \mathcal{L} \frac{\frac{1}{P} \oint - \frac{\partial T}{\partial n} \Big|_w ds}{\frac{1}{P} \oint T_w ds - \frac{1}{\bar{w}A} \int \int_A wT dA} \quad (11)$$

where $\partial T/\partial n$ represents the temperature gradient at the duct wall with respect to an inward directed normal, ds is the differential of arc length, \mathcal{L} is an arbitrary characteristic length scale to be determined later, A is the cross-sectional area and P is the wetted perimeter of the duct. Traditionally, $\mathcal{L} = 4A/P$, the hydraulic diameter of the duct. Finally, the flow length averaged Nusselt number is related to the local Nusselt number through

$$\bar{Nu} = \frac{1}{z} \int_0^z Nu(z) dz \quad (12)$$

Literature Review

A review of the literature reveals that very little work has been done in the area of modeling heat transfer in the combined entrance region of non-circular ducts. Only the circular duct and parallel plate channel have models or correlations which cover a wide range of Prandtl number and dimensionless duct length. Even for these common channel shapes, the expressions are only valid for particular boundary conditions and flow conditions.

Stephan, see [3], developed a correlation for the circular tube which is valid for all values of the dimensionless duct length z^* and for $0.1 < Pr < \infty$.

The Stephan correlation (see [3]) has the following form:

$$Nu_{m,T} = \frac{Nu(Pr \rightarrow \infty)}{\tanh(2.432Pr^{1/6}(z^*)^{1/6})} \quad (13)$$

where

$$Nu(Pr \rightarrow \infty) = \frac{3.657}{\tanh(2.264(z^*)^{1/3} + 1.7(z^*)^{2/3})} + \frac{0.0499}{z^*} \tanh(z^*) \quad (14)$$

A solution for the circular tube based upon the Karman-Pohlhausen integral method was first developed by Kays [13] and later corrected by Kreith [14]. It is given by the following expression which is only valid for small values of the parameter z^* :

$$Nu_{m,T} = \frac{1}{4z^*} \ln \left(\frac{1}{1 - 2.65(z^*)^{1/2} Pr^{-1/6}} \right) \quad (15)$$

which is valid for $Pr > 2$ and $z^* < 0.001$.

For the case of a parallel plate channel, Stephan [4] correlated numerical results in the following way:

$$Nu_{m,T} = 7.55 + \frac{0.024(z^*)^{-1.14}}{1 + 0.0358Pr^{0.17}(z^*)^{-0.64}} \quad (16)$$

which is valid for $0.1 < Pr < 1000$. Shah and Bhatti, see Ref. [8], obtained the following expression for the local Nusselt number from the correlation developed by Stephan [4]

$$Nu_{z,T} = 7.55 + \frac{0.024(z^*)^{-1.14}(0.0179Pr^{0.17}(z^*)^{-0.64} - 0.14)}{(1 + 0.0358Pr^{0.17}(z^*)^{-0.64})^2} \quad (17)$$

Sparrow [15] using the Karman-Pohlhausen integral method, obtained the following approximate analytical expression for the Nusselt number

$$Nu_{m,T} = \frac{0.664}{\sqrt{z^*} Pr^{1/6}} (1 + 6.27(Prz^*)^{4/9})^{1/2} \quad (18)$$

which is valid for $Pr > 2$ and $z^* < 0.001$.

Churchill and Ozoe [1,2] developed Eqs. (19,20), for the local Nusselt number for the UWF and UWT conditions, where $Gz = \pi/(4z^*)$ is the Graetz number, in the combined entrance region of a circular duct. These models were developed using the asymptotic correlation method of Churchill and Usagi [11] and are valid for all Prandtl numbers $0 < Pr < \infty$, but only for the circular duct.

$$\frac{Nu_{z,T} + 1.7}{5.357[1 + (Gz/97)^{8/9}]^{3/8}} = \left[1 + \left(\frac{Gz/71}{[1 + (Pr/0.0468)^{2/3}]^{1/2} [1 + (Gz/97)^{8/9}]^{3/4}} \right)^{4/3} \right]^{3/8} \quad (19)$$

$$\frac{Nu_{z,H} + 1}{5.364[1 + (Gz/55)^{10/9}]^{3/10}} = \left[1 + \left(\frac{Gz/28.8}{[1 + (Pr/0.0207)^{2/3}]^{1/2} [1 + (Gz/55)^{10/9}]^{3/5}} \right)^{5/3} \right]^{3/10} \quad (20)$$

In all of the above models, the characteristic length is $\mathcal{L} = D_h$. Later it will be shown that a more appropriate length scale should be used.

Only a limited set of numerical data are available for the combined entrance region. In addition to numerical data for the circular duct and the parallel plate channel for a range of Prandtl numbers, a small set of data are available for the rectangular and triangle ducts for $Pr = 0.72$. All of the available data and models for the combined entrance region are reviewed by Kakac and Yener [10].

Finally, numerical data were obtained by Asako et al. [6] for the polygonal ducts for a range of Prandtl numbers, while Garimella et al. [5] obtained empirical data for the rectangular channel in the laminar-transition-turbulent regions for a number of aspect ratios.

At present, no single model is available which can predict the data for both the circular duct or parallel plate channel. Further, no

correlating equations are available for any of the numerical data related to non-circular ducts. In the sections which follow, a new model is proposed which serves these needs.

Model Development

A model which is valid for most non-circular ducts will now be developed using an approach similar to that proposed by Churchill and Ozoe [1,2]. Churchill and Ozoe [1,2] developed a model for the circular duct which is valid for all Prandtl numbers over the entire range of dimensionless duct lengths, by combining a composite model for the Graetz problem with a composite model for laminar forced convection from a flat plate. With some additional modification, Churchill and Ozoe [1,2] were able to apply these models for all Prandtl numbers. The present approach is limited to the range $0.1 < Pr < \infty$, which is valid for most flows found in heat exchangers.

The model development will be presented in several steps. First, each characteristic region: fully developed flow ($L \gg L_h, L_t$), Graetz flow ($L \gg L_h, L \ll L_t$), and laminar boundary layer flow ($L \ll L_h, L_t$) will be examined in detail to show how each region is dealt with in non-circular ducts. Next a model is developed for a range of Prandtl numbers, duct lengths, thermal boundary condition, and Nusselt number type, i.e., local or average value. Finally, the model is compared with published data from numerous sources. Much of these data have been collected and organized by Shah and London [7]. Since much of the published data appears in graphical form in the original sources, tabulated values from [7] are used for comparison. In most cases these data were obtained from the original authors, when available.

Fully Developed Flow. The fully developed flow limit for both hydrodynamic and thermal problems has been addressed by Muzychka [16] and reported in Yovanovich and Muzychka [17] and Muzychka and Yovanovich [18,19]. Additional results appear in Muzychka and Yovanovich [20,21] and Yovanovich et al. [22]. These references [17–22] provide models for the classic Graetz problem and the hydrodynamic entrance problem for forced flow, and for natural convection in vertical ducts of non-circular cross-section. In addition, Refs. [20], [21] applied scaling principles to all of the fundamental internal flow problems.

An important result of Yovanovich and Muzychka [17] is that the characteristic length scale for non-circular ducts in laminar flows should not be the hydraulic diameter, but rather, the square root of the cross-sectional area of the duct. This conclusion was drawn from dimensional analysis performed on an arbitrarily shaped duct with validation provided by examination of the analytical and numerical data from the literature. Bejan [23] also arrived at the same conclusion using his constructal theory of organization in nature.

Yovanovich and Muzychka [17] showed that when the friction factor-Reynolds number product is based upon the square root of cross-sectional area, the vast number of data were reduced to a single curve which was merely a function of the aspect ratio of the duct or channel. They also showed that this curve was accurately represented by the first term of the exact series solution for the rectangular duct cross-section. This result is given by

$$f Re_{\sqrt{A}} = \frac{12}{\sqrt{\epsilon}(1+\epsilon) \left[1 - \frac{192\epsilon}{\pi^5} \tanh\left(\frac{\pi}{2\epsilon}\right) \right]} \quad (21)$$

For most rectangular channels it is sufficient to choose $0.01 < \epsilon < 1$, since the rectangular channel approaches the parallel plate for $\epsilon < 0.01$. A plot of this model with data for many duct shapes is provided in Fig. 1. Figure 2 shows a broader comparison with several other non-circular ducts.

The aspect ratio in Figs. 1 and 2 is taken to be a measure of the slenderness of the non-circular duct. In most cases, it is merely the width to length ratio of the duct. However, in cases such as the circular annulus, annular sector, and the trapezoid, it is defined as

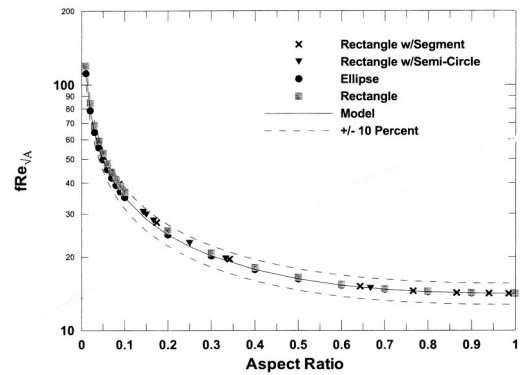


Fig. 1 $f Re_{\sqrt{A}}$ for singly connected geometries, data from Ref. [7]

the mean channel spacing divided by the mean channel width. This alternative definition was chosen since these shapes contain the parallel plate channel limit when aspect ratio becomes small.

Next, Muzychka and Yovanovich [18] applied the same reasoning to the fully developed Nusselt number in non-circular ducts, leading to the development of a model for the classic Graetz problem.

Figures 3 and 4 compare the data for many duct shapes obtained from Shah and London [7]. When the results are based upon the square root of cross-sectional area two distinct bounds are formed for the Nusselt number. The lower bound consists of all duct shapes which have re-entrant corners, i.e., angles less than 90 deg, while the upper bound consists of all ducts with rounded corners and/or right angled corners. A model has been developed

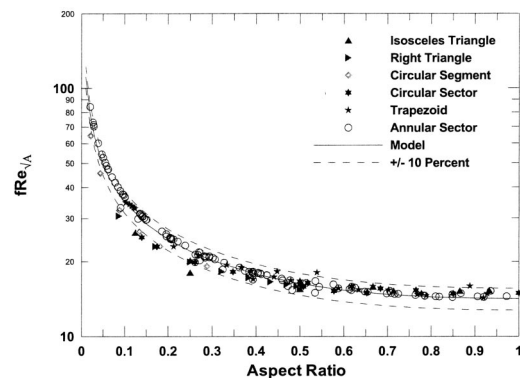


Fig. 2 $f Re_{\sqrt{A}}$ for other singly connected geometries, data from Ref. [7]

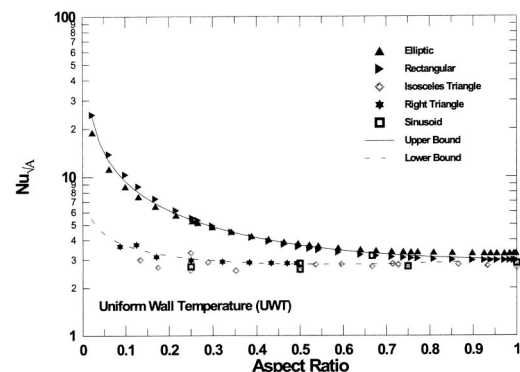


Fig. 3 Fully developed flow Nu_T , data from Ref. [7]

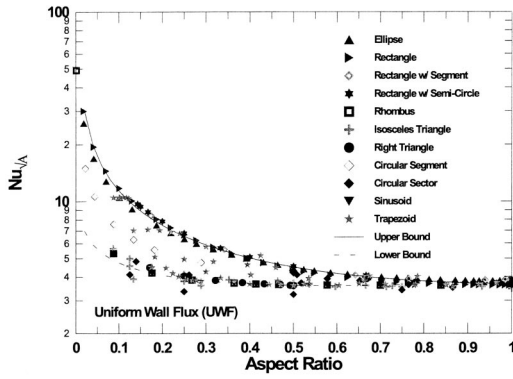


Fig. 4 Fully developed flow $Nu_{\sqrt{A}}$, data from Ref. [7]

which accurately predicts the data for both thermal boundary conditions and both upper and lower bounds. The resulting expression which is related to Eq. (21) is

$$Nu_{\sqrt{A}} = C_1 \left(\frac{f Re_{\sqrt{A}}}{8 \sqrt{\pi} \epsilon^\gamma} \right) \quad (22)$$

where C_1 is equal to 3.24 for the (UWT) boundary condition and 3.86 for the (UWF) boundary condition. These results are the exact solutions for fully developed flow in a circular tube when the characteristic length scale is the square root of cross-sectional area. The parameter γ is chosen based upon the geometry. Values for γ which define the upper and lower bounds in Figs. 3 and 4 are fixed at $\gamma = 1/10$ and $\gamma = -3/10$, respectively. Almost all of the available data are predicted within ± 10 percent by Eq. (22), with a few exceptions.

Graetz Flow. If the velocity distribution is fully developed and the temperature distribution is allowed to develop, the classic Graetz problem results. In the thermal entrance region, the results are weak functions of the shape and geometry of the duct. This behavior is characterized by the following approximate analytical expression first attributed to Leveque, see [24]:

$$Nu \propto \left(\frac{C^*}{z^*} \right)^{1/3} \quad (23)$$

where C^* is the dimensionless mean velocity gradient at the duct wall and z^* is the dimensionless axial location. Thus, if C^* is made a weak function of shape, then Nu will be a weaker function of shape due to the one third power.

In the thermal entrance region of non-circular ducts the thermal boundary layer is thin and it may be assumed to be developing in a region where the velocity gradient is linear. For very small distances from the duct inlet, the effect of curvature on the boundary layer development is negligible. Thus, we may treat the duct wall as a flat plate. The governing equation for this situation is given by

$$C y \frac{\partial T}{\partial z} = \alpha \frac{\partial^2 T}{\partial y^2} \quad (24)$$

where the constant C represents the mean velocity gradient at the duct wall. For non-circular ducts, this constant is defined as:

$$C = \left. \frac{\partial w}{\partial n} \right|_w = \frac{1}{P} \oint \left. \frac{\partial w}{\partial n} \right|_w ds \quad (25)$$

For hydrodynamically fully developed flow, the constant C is related to the friction factor-Reynolds number product

$$\frac{f Re_{\mathcal{L}}}{2} = \left. \frac{\partial w}{\partial n} \right|_w \frac{\mathcal{L}}{\bar{w}} = C^* \quad (26)$$

where \mathcal{L} is an arbitrary length scale.

If the following parameters are defined:

$$\bar{y} = \frac{y}{\mathcal{L}} \quad z^* = \frac{z/\mathcal{L}}{Re_{\mathcal{L}} Pr} \quad \theta = T - T_o \quad Re_{\mathcal{L}} = \frac{\bar{w} \mathcal{L}}{\nu}$$

the governing equation becomes

$$C^* \bar{y} \frac{\partial \theta}{\partial z^*} = \frac{\partial^2 \theta}{\partial \bar{y}^2} \quad (27)$$

The governing equation may now be transformed into an ordinary differential equation for each wall condition using a similarity variable [22]

$$\eta = \frac{\bar{y}}{(9z^*/C^*)^{1/3}} \quad (28)$$

Both the UWT and UWF conditions are examined. Solution to the Leveque problem is discussed in Bird et al. [24]. The solution for local Nusselt number with the UWT condition yields:

$$Nu_{\mathcal{L}} = \frac{3\sqrt{3} \Gamma(2/3)}{2 \pi} \left(\frac{f Re_{\mathcal{L}}}{18z^*} \right)^{1/3} \approx 0.4273 \left(\frac{f Re_{\mathcal{L}}}{z^*} \right)^{1/3} \quad (29)$$

while the solution for the local Nusselt number for the (UWF) condition yields:

$$Nu_{\mathcal{L}} = \Gamma(2/3) \left(\frac{f Re_{\mathcal{L}}}{18z^*} \right)^{1/3} \approx 0.5167 \left(\frac{f Re_{\mathcal{L}}}{z^*} \right)^{1/3} \quad (30)$$

The average Nusselt number for both cases may be obtained from Eq. (12), which gives

$$\overline{Nu}_{\mathcal{L}} = \frac{3}{2} Nu_{\mathcal{L}} \quad (31)$$

The solution for each wall condition may now be compactly written as

$$Nu_{\mathcal{L}} = C_2 C_3 \left(\frac{f Re_{\mathcal{L}}}{z^*} \right)^{1/3} \quad (32)$$

where the value of C_2 is 1 for local conditions and 3/2 for average conditions, and C_3 takes a value of 0.427 for UWT and 0.517 for UWF.

The Leveque approximation is valid where the thermal boundary layer develops in the region near the wall where the velocity profile is linear. The weak effect of duct geometry in the entrance region is due to the presence of the friction factor-Reynolds number product, $f Re$, in the above expression, which is representative of the average velocity gradient at the duct wall. The typical range of the $f Re$ group is $6.5 < f Re_{D_h} < 24$, Shah and London [7]. This results in $1.87 < (f Re_{D_h})^{1/3} < 2.88$, which illustrates the weak dependency of the thermal entrance region on shape and aspect ratio. Further reductions are achieved for similar shaped ducts by using the length scale $\mathcal{L} = \sqrt{A}$, i.e., see Figs. 1 and 2.

A model which is valid over the entire range of dimensionless duct lengths for $Pr \rightarrow \infty$, was developed by Muzychka and Yovanovich [18] by combining Eq. (22) with Eq. (32) using the Churchill and Usagi [11] asymptotic correlation method. The form of the proposed model for an arbitrary characteristic length scale is

$$Nu(z^*) = \left(\left\{ C_2 C_3 \left(\frac{f Re}{z^*} \right)^{1/3} \right\}^n + (Nu_{fd})^n \right)^{1/n} \quad (33)$$

Now using the result for the fully developed friction factor, Eq. (21), and the result for the fully developed flow Nusselt number, Eq. (22), with $n \approx 5$ a new model [19] was proposed having the form

Table 1 Coefficients for general model

Boundary Condition		
UWT	$C_3=0.409, C_1=3.24$	$f(\text{Pr}) = \frac{0.564}{[1 + (1.664\text{Pr}^{1/6})^{9/2}]^{2/9}}$
UWF	$C_3=0.501, C_1=3.86$	$f(\text{Pr}) = \frac{0.886}{[1 + (1.909\text{Pr}^{1/6})^{9/2}]^{2/9}}$
Nusselt Number Type		
Local	$C_2=1$	$C_4=1$
Average	$C_2=3/2$	$C_4=2$
Shape Parameter		
Upper Bound	$\gamma=1/10$	
Lower Bound	$\gamma=-3/10$	

$$\text{Nu}_{\sqrt{A}}(z^*) = \left[\left\{ C_2 C_3 \left(\frac{f \text{Re}_{\sqrt{A}}}{z^*} \right)^{1/3} \right\}^5 + \left\{ C_1 \left(\frac{f \text{Re}_{\sqrt{A}}}{8 \sqrt{\pi} \epsilon^\gamma} \right) \right\}^5 \right]^{1/5} \quad (34)$$

where the constants $C_1, C_2, C_3,$ and γ are given in Table 1. These constants define the various cases for local or average Nusselt number and isothermal or isoflux boundary conditions for the Graetz problem. The constant C_3 was adjusted from that found by the Leveque approximation to provide better agreement with the data.

Laminar Boundary Layer Flow. Finally, if both hydrodynamic and thermal boundary layers develop simultaneously, the results are strong functions of the fluid Prandtl number. In the combined entrance region the behavior for very small values of z^* may be adequately modeled by treating the duct wall as a flat plate. The characteristics of this region are

$$\text{Pr} \rightarrow 0 \quad \frac{\text{Nu}_z}{\sqrt{\text{Re}_z}} = 0.564 \text{Pr}^{1/2} \quad (35)$$

$$\text{Pr} \rightarrow \infty \quad \frac{\text{Nu}_z}{\sqrt{\text{Re}_z}} = 0.339 \text{Pr}^{1/3} \quad (36)$$

for the UWT condition [2], and

$$\text{Pr} \rightarrow 0 \quad \frac{\text{Nu}_z}{\sqrt{\text{Re}_z}} = 0.886 \text{Pr}^{1/2} \quad (37)$$

$$\text{Pr} \rightarrow \infty \quad \frac{\text{Nu}_z}{\sqrt{\text{Re}_z}} = 0.464 \text{Pr}^{1/3} \quad (38)$$

for the UWF condition [1].

Composite models for each wall condition were developed by Churchill and Ozoe [1,2] using the asymptotic correlation method of Churchill and Usagi [11]. The results may be developed in terms of the $\text{Pr} \rightarrow 0$ behavior or the $\text{Pr} \rightarrow \infty$ behavior. For internal flow problems, the appropriate form is chosen to be in terms of the $\text{Pr} \rightarrow 0$ characteristic which introduces the Peclet number $\text{Pe} = \text{Re Pr}$:

$$\frac{\text{Nu}_z}{(\text{Re}_z \text{Pr})^{1/2}} = \frac{C_o}{\left[1 + \left(\frac{C_o \text{Pr}^{1/6}}{C_\infty} \right)^n \right]^{1/n}} = f(\text{Pr}) \quad (39)$$

where C_o and C_∞ represent the coefficients of the right hand side of Eqs. (35–38). The correlation parameter n may be found by solving Eq. (39) at an intermediate value of Pr where the exact solution is known, i.e., $\text{Pr} = 1$. This leads to $n = 4.537$ for the UWT condition and $n = 4.598$ for the UWF condition. For simplicity, $n = 9/2$ is chosen for both cases.

The average Nusselt number for both cases may now be obtained from Eq. (12), which gives:

$$\overline{\text{Nu}}_L = 2 \text{Nu}_L \quad (40)$$

The solution for each wall condition may now be compactly written as

$$\text{Nu}_L = \frac{C_4}{\sqrt{z^*}} f(\text{Pr}) \quad (41)$$

where the value of $C_4 = 1$ for local conditions and $C_4 = 2$ for average conditions, and $f(\text{Pr})$ are defined as

$$f(\text{Pr}) = \frac{0.564}{[1 + (1.664\text{Pr}^{1/6})^{9/2}]^{2/9}} \quad (42)$$

for the UWT condition, and

$$f(\text{Pr}) = \frac{0.886}{[1 + (1.909\text{Pr}^{1/6})^{9/2}]^{2/9}} \quad (43)$$

for the UWF condition. The preceding results are valid only for small values of the parameter z^* .

General Model. A new model for the combined entrance region may now developed by combining the solution for a flat plate with the model for the Graetz flow problem developed earlier. The proposed model takes the form

$$y(z) = (\{y_{z \rightarrow 0}(\text{Pr})\}^m + \{y_{z \rightarrow \infty}^n + y_{z \rightarrow \infty}^n\}^{m/n})^{1/m} \quad (44)$$

which is similar to that proposed by Churchill and Ozoe [1,2] for the circular duct. This model is a composite solution of the three asymptotic solutions just discussed.

This results in the following model for simultaneously developing flow in a duct of arbitrary cross-sectional shape

$$\text{Nu}_{\sqrt{A}}(z^*) = \left[\left(\frac{C_4 f(\text{Pr})}{\sqrt{z^*}} \right)^m + \left(\left\{ C_2 C_3 \left(\frac{f \text{Re}_{\sqrt{A}}}{z^*} \right)^{1/3} \right\}^5 + \left\{ C_1 \left(\frac{f \text{Re}_{\sqrt{A}}}{8 \sqrt{\pi} \epsilon^\gamma} \right) \right\}^5 \right)^{m/5} \right]^{1/m} \quad (45)$$

The parameter m was determined to vary between 2 and 7 for all of the data examined. Values for the blending parameter were found to be weak functions of the duct aspect ratio and whether a local or average Nusselt number was examined. However, the blending parameter was found to be most dependent upon the fluid Prandtl number.

A simple linear approximation was determined to provide better accuracy than choosing a single value for all duct shapes. Due to the variation in geometries and data, higher order approximations offered no additional advantage. Therefore, the linear approxima-

tion which predicts the blending parameter within 30 percent was found to be satisfactory. Variations in the blending parameter of this order will lead to small errors in the model predictions, whereas variations on the order of 100 percent or more, i.e., choosing a fixed value, produce significantly larger errors. The resulting fit for the blending parameter m is

$$m = 2.27 + 1.65Pr^{1/3} \quad (46)$$

The above model is valid for $0.1 < Pr < \infty$ which is typical for most low Reynolds number flow heat exchanger applications.

Finally, the following model was developed by Muzychka and Yovanovich [18,20] for the apparent friction factor in the entrance region. It is given here for completeness as follows:

$$f_{app} Re_{\sqrt{A}} = \left[\left(\frac{12}{\sqrt{\epsilon}(1+\epsilon) \left[1 - \frac{192\epsilon}{\pi^5} \tanh\left(\frac{\pi}{2\epsilon}\right) \right]} \right)^2 + \left(\frac{3.44}{\sqrt{z^+}} \right)^2 \right]^{1/2} \quad (47)$$

It predicts most of the non-circular friction data within ± 10 percent.

Comparisons of Model With Data

Comparisons with the available data from [7] are provided in Tables 2–6 and Figs. 5–11. Good agreement is obtained with the data for the circular duct and parallel plate channel. Note that comparison of the model for the parallel plate channel was obtained by considering a rectangular duct having an aspect ratio of $\epsilon = 0.01$. This represents a reasonable approximation for this system. The data are also compared with the models of Churchill and Ozoe [1,2] and Stephan [3,4] for the circular duct and parallel plate channel in Figs. 5–8.

The model is compared with the data by determining the percent difference between the data and the model predictions. Maximum and minimum values of the percent difference are given in Tables 2–6 for each set of data.

The numerical data for the the UWT circular duct fall short of the model predictions at low Pr numbers. However, all of the models are in excellent agreement with the integral formulation of

Table 2 Comparison of model and data for circular duct [7] (min/max—% diff)

Pr	$Nu_{z,T}$	$Nu_{m,T}$	$Nu_{z,H}$
0.7	-6.59/-0.07	-14.69/3.87	-0.08/3.98
2.0	-8.43/-0.07	-19.07/1.34	-0.07/5.19
5.0	-8.65/-0.07	-24.41/-0.60	-0.20/5.40
∞		-1.24/8.57	-1.60/5.27

Table 3 Comparison of model and data for parallel plate channel [7] (min/max—% diff)

Pr	$Nu_{m,T}$	$Nu_{z,H}$
0.1	-13.33/6.32	N/A
0.7	-5.17/7.43	-1.59/5.32
2.0	-0.24/7.43	-1.79/4.49
5.0	-0.02/13.75	-0.05/6.01
∞	1.60/10.0	-9.93/7.03

Table 4 Comparison of model and data for square duct [7] (min/max—% diff)

Pr	$Nu_{z,H}$	$Nu_{m,H}$
0.1	-0.45/11.32	-8.14/11.42
1.0	-2.19/2.56	-6.72/4.82
10	-1.96/1.52	-1.15/5.07
∞	-2.76/1.73	

Table 5 Comparison of model and data for rectangular duct [7]: Pr=0.72, (min/max—% diff)

$\epsilon = b/a$	$Nu_{m,T}$	$Nu_{z,H}$	$Nu_{m,H}$
1	-20.7/1.21	-0.18/13.14	-3.75/14.8
1/2	-18.5/7.48	-0.11/13.13	-2.42/14.6
1/3	-16.5/7.43	-0.05/13.4	-0.42/13.16
1/4	-14.6/6.73	-0.04/12.04	-0.33/13.5

Table 6 Comparison of model and data for equilateral triangular ducts [7] (min/max—% diff)

Pr	$Nu_{z,T}$	$Nu_{m,T}$	$Nu_{z,H}$	$Nu_{m,H}$
0.72	-14.17/-1.85	-11.1/12.27	-1.50/4.19	-8.92/4.84
∞		-12.11/-6.81	-7.24/-2.09	

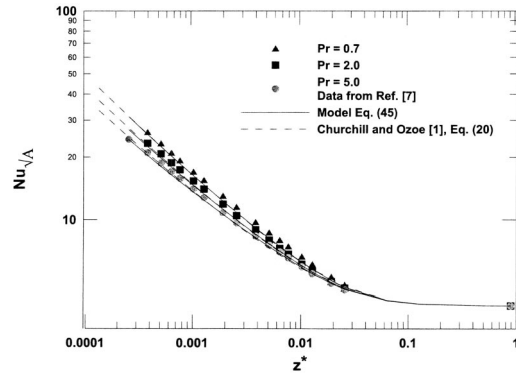


Fig. 5 Simultaneously developing flow in a circular tube $Nu_{H,z}$, data from Ref. [7]

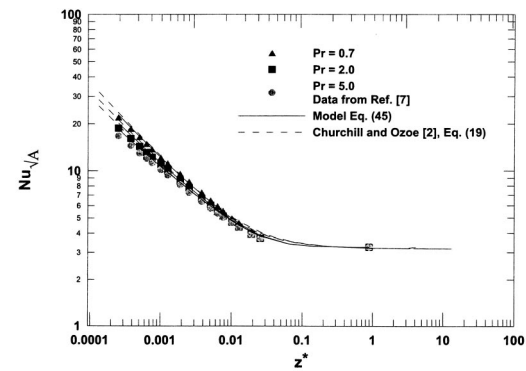


Fig. 6 Simultaneously developing flow in a circular tube $Nu_{T,z}$, data from Ref. [7]

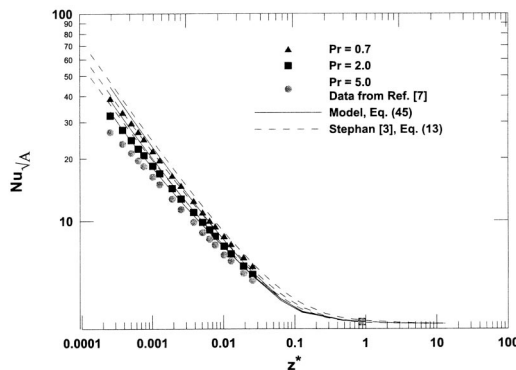


Fig. 7 Simultaneously developing flow in a circular tube $Nu_{T,m}$, data from Ref. [7]

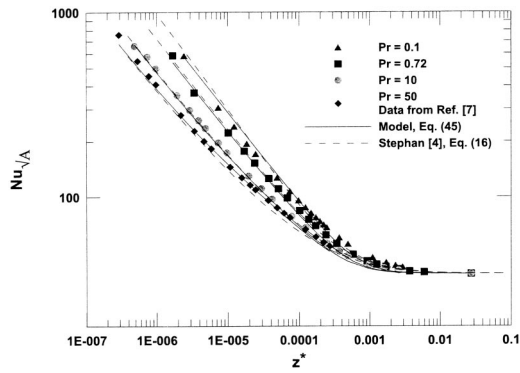


Fig. 8 Simultaneously developing flow in channel $Nu_{T,m}$, data from Ref. [7]

Kreith [14]. Good agreement is also obtained for the case of the square duct for all Prandtl numbers. Comparisons of the model with data for the rectangular duct at various aspect ratios, see Table 5, and the equilateral triangular duct, see Table 6, show that larger discrepancies arise. Also included in Tables 2–6 are the results of Muzychka and Yovanovich [19] for the case of $Pr \rightarrow \infty$.

The data used for comparison in Tables 5 and 6 were obtained by Wibulswas [25]. In this work, the effects of transverse velocities in both the momentum and energy equations were ignored. Comparison of the data for the square duct at $Pr = 1.0$ obtained by Chandrupatla and Sastri [26] which includes the effects of trans-

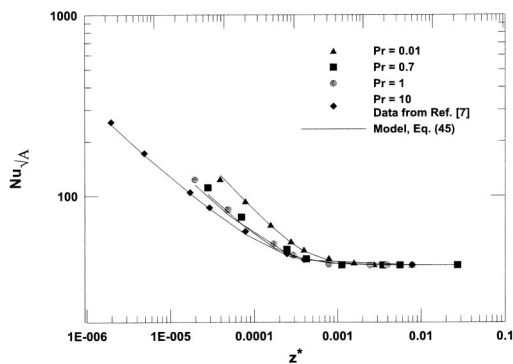


Fig. 9 Simultaneously developing flow in channel $Nu_{H,z}$, data from Ref. [7]

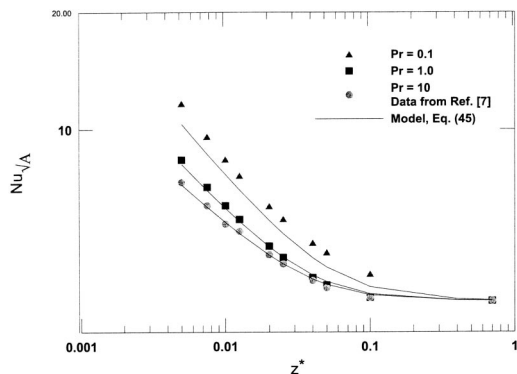


Fig. 10 Simultaneously developing flow in square duct $Nu_{H,z}$, data from Ref. [7]

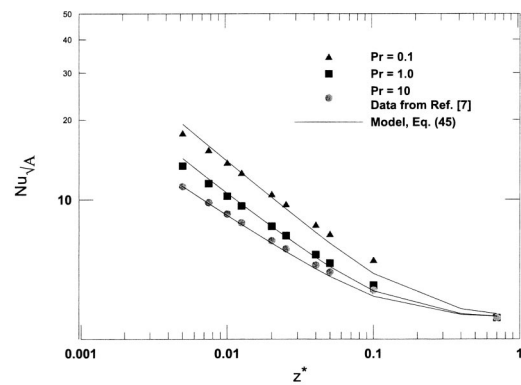


Fig. 11 Simultaneously developing flow in square duct $Nu_{H,m}$, data from Ref. [7]

verse velocities with the data of Wibulswas [25] for $Pr = 0.72$ shows that the discrepancy is likely due to the data and not the model.

The accuracy for each case may be improved considerably by using the optimal value of the parameter m . However, this introduces an additional parameter into the model which is deemed unnecessary for purposes of heat exchanger design. The proposed model predicts most of the available data for the combined entry problem to within ± 15 percent and may be used to predict the heat transfer characteristics for other non-circular ducts for which there are presently no data.

The present model also agrees well with the published models of Churchill and Ozoe [1,2], Eqs. (19,20), and the models of Stephan [3,4], Eqs. (13,16), for the tube and channel. It is evident from Figs. 5–8 that the present model provides equal or better accuracy to the existing expressions.

Summary and Conclusions

A general model for predicting the heat transfer co-efficient in the combined entry region of non-circular ducts was developed. This model is valid for $0.1 < Pr < \infty$, $0 < z^* < \infty$, both uniform wall temperature (UWT) and uniform wall flux (UWF) conditions, and for local and mean Nusselt numbers. Model predictions agree with numerical data to within ± 15 percent for most non-circular ducts and channels. The model was developed by combining the asymptotic results of laminar boundary layer flow and Graetz flow for the thermal entrance region. In addition, by means of a novel characteristic length, the square root of cross-sectional area, results for many non-circular ducts of similar aspect ratio collapse onto a single curve.

Acknowledgments

The authors acknowledge the support of the Natural Sciences and Engineering Research Council of Canada (NSERC) under a post-doctoral research fellowship for the first author and research grants for both authors.

Nomenclature

- A = flow area, m^2
- a = major axis of ellipse or rectangle, m
- b = minor axis of ellipse or rectangle, m
- C = constant
- C_i = constants, $i = 1..5$
- D = diameter of circular duct, m
- D_h = hydraulic diameter of plain channel, $\equiv 4A/P$
- f = friction factor $\equiv \bar{\tau}/(1/2\rho\bar{v}^2)$
- Gz = Graetz number, $\equiv \pi/4z^*$
- h = heat transfer coefficient, W/m^2K

k = thermal conductivity, W/mK
 L = length of channel, m
 L_h = hydrodynamic entry length, m
 L_t = thermal entry length, m
 L^* = dimensionless thermal length, $\equiv L/\mathcal{L} Re_{\mathcal{L}} Pr$
 \mathcal{L} = characteristic length scale, m
 m = correlation parameter
 \dot{m} = mass flow rate, kg/s
 n = inward directed normal
 $Nu_{\mathcal{L}}$ = Nusselt number, $\equiv h\mathcal{L}/k$
 P = perimeter, m
 p = pressure, Pa
 Pr = Prandtl number, $\equiv \nu/\alpha$
 q = heat flux, W/m^2
 Q = heat transfer rate, W
 r = radius, m
 $Re_{\mathcal{L}}$ = Reynolds number, $\equiv \bar{w}\mathcal{L}/\nu$
 s = arc length, m
 T = temperature, K
 T_m = bulk temperature, K
 T_w = wall temperature, K
 u, v, w = velocity components, m/s
 w = axial velocity, m/s
 \bar{w} = average velocity, m/s
 x, y, z = cartesian coordinates, m
 z = axial coordinate, m
 z^+ = dimensionless position for hydrodynamically developing flows, $\equiv z/\mathcal{L} Re_{\mathcal{L}}$
 z^* = dimensionless position for thermally developing flows, $\equiv z/\mathcal{L} Re_{\mathcal{L}} Pr$

Greek Symbols

α = thermal diffusivity, m^2/s
 ϵ = aspect ratio, $\equiv b/a$
 γ = shape parameter
 $\Gamma(\cdot)$ = Gamma function
 μ = dynamic viscosity, Ns/m^2
 ν = kinematic viscosity, m^2/s
 ρ = fluid density, kg/m^3
 τ = wall shear stress, N/m^2
 θ = temperature excess, $T - T_b$, K

References

- [1] Churchill, S. W., and Ozoe, H., 1973, "Correlations for Laminar Forced Convection with Uniform Heating in Flow Over a Plate and in Developing and Fully Developed Flow in a Tube," *ASME J. Heat Transfer*, **95**, pp. 78–84.
- [2] Churchill, S. W., and Ozoe, H., 1973, "Correlations for Laminar Forced Convection in Flow Over an Isothermal Flat Plate and in Developing and Fully Developed Flow in an Isothermal Tube," *ASME J. Heat Transfer*, **95**, pp. 416–419.
- [3] Baehr, H., and Stephan, K., 1998, *Heat Transfer*, Springer-Verlag.
- [4] Stephan, K., 1959, "Warmeubergang und Druckabfall bei Nicht Ausgebildeter Laminar Stromung in Rohren und in Ebenen Spalten," *Chem-Ing-Tech*, **31**, pp. 773–778.
- [5] Garimella, S., Dowling, W. J., Van derVeen, M., Killion, J., 2000, "Heat Transfer Coefficients for Simultaneously Developing Flow in Rectangular Tubes," *Proceedings of the 2000 International Mechanical Engineering Congress and Exposition*, Vol. 2, pp. 3–11.
- [6] Asako, Y., Nakamura, H., and Faghri, M., 1988, "Developing Laminar Flow and Heat Transfer in the Entrance Region of Regular Polygonal Ducts," *Int. J. Heat Mass Transfer*, **31**, pp. 2590–2593.
- [7] Shah, R. K., and London, A. L., 1978, *Laminar Flow Forced Convection in Ducts*, Academic Press, New York, NY.
- [8] Kakac, S., Shah, R. K., and Aung, W., 1987, *Handbook of Single Phase Convective Heat Transfer*, Wiley, New York.
- [9] Rohsenow, W. M., Hartnett, J. P., and Cho, Y. I., eds., 1988, *Handbook of Heat Transfer*, McGraw-Hill, New York.
- [10] Kakac, S., and Yener, Y., 1983, "Laminar Forced Convection in the Combined Entrance Region of Ducts," in *Low Reynolds Number Heat Exchangers*, S. Kakac, R. K. Shah and A. E. Bergles, eds., Hemisphere Publishing, Washington, pp. 165–204.
- [11] Churchill, S. W., and Usagi, R., 1972, "A General Expression for the Correlation of Rates of Transfer and Other Phenomena," *American Institute of Chemical Engineers*, **18**, pp. 1121–1128.
- [12] Kays, W. M., and Crawford, M. E., 1993, *Convective Heat and Mass Transfer*, McGraw-Hill, New York, NY.
- [13] Kays, W. M., 1955, "Numerical Solutions for Laminar Flow Heat Transfer in Circular Tubes," *Trans. ASME*, **77**, pp. 1265–1274.
- [14] Kreith, F., 1965, *Principles of Heat Transfer*, 2nd ed., International Textbook Co., Scranton, PA.
- [15] Sparrow, E. M., 1955, "Analysis of Laminar Forced Convection Heat Transfer in Entrance Region of Flat Rectangular Ducts," *NACA Technical Note 3331*.
- [16] Muzychka, Y. S., 1999, "Analytical and Experimental Study of Fluid Friction and Heat Transfer in Low Reynolds Number Flow Heat Exchangers," Ph.D. thesis, University of Waterloo, Waterloo, ON.
- [17] Yovanovich, M. M., and Muzychka, Y. S., 1997, "Solutions of Poisson Equation within Singly and Doubly Connected Domains," AIAA Paper 97-3880, presented at the National Heat Transfer Conference, Baltimore MD.
- [18] Muzychka, Y. S., and Yovanovich, M. M., 1998, "Modeling Friction Factors in Non-Circular Ducts for Developing Laminar Flow," AIAA Paper 98-2492, presented at the 2nd Theoretical Fluid Mechanics Meeting, Albuquerque, NM.
- [19] Muzychka, Y. S., and Yovanovich, M. M., 1998, "Modeling Nusselt Numbers for Thermally Developing Laminar Flow in Non-Circular Ducts," AIAA Paper 98-2586, presented at the 7th AIAA/ASME Joint Thermophysics and Heat Transfer Conference, Albuquerque, NM.
- [20] Muzychka, Y. S., and Yovanovich, M. M., 2002, "Laminar Flow Friction and Heat Transfer in Non-Circular Ducts and Channels: Part I—Hydrodynamic Problem," *Compact Heat Exchangers: A Festschrift on the 60th Birthday of Ramesh K. Shah*, Grenoble, France, August 24, 2002, G. P. Celata, B. Thonon, A. Bontemps, and S. Kandlikar, eds., pp. 123–130.
- [21] Muzychka, Y. S., and Yovanovich, M. M., 2002, "Laminar Flow Friction and Heat Transfer in Non-Circular Ducts and Channels: Part II—Thermal Problem," *Compact Heat Exchangers: A Festschrift on the 60th Birthday of Ramesh K. Shah*, Grenoble, France, August 24, 2002, G. P. Celata, B. Thonon, A. Bontemps, and S. Kandlikar, eds., pp. 131–139.
- [22] Yovanovich, M. M., Teertstra, P. M., and Muzychka, Y. S., 2001, "Natural Convection Inside Vertical Isothermal Ducts of Constant Arbitrary Cross-Section," AIAA Paper 01-0368, presented at the 39th Aerospace Sciences Meeting and Exhibit, Reno, NV, January 8–11.
- [23] Bejan, A., 2000, *Shape and Structure, From Engineering to Nature*, Cambridge University Press, Cambridge, UK.
- [24] Bird, R. B., Stewart, W. E., and Lightfoot, E. N., 1960, *Transport Phenomena*, Wiley, New York, NY.
- [25] Wibuswas, P., 1966, "Laminar Flow Heat Transfer in Noncircular Ducts," Ph.D. thesis, London University.
- [26] Chandrupatla, A. R., and Sastri, V. M. K., 1977, "Laminar Forced Convection Heat Transfer of a Non-Newtonian Fluid in a Square Duct," *Int. J. Heat Mass Transfer*, **20**, pp. 1315–1324.